Fatigue of Welded Connections in Extruded Aluminium Hollow Section Profiles

K A Macdonald[a], P J Haagensen[b]

[a] University of Stavanger, 4036 STAVANGER, Norway
[b] Norwegian University of Science and Technology, 7491 TRONDHEIM, Norway

Abstract This paper presents a study of the fatigue properties of welded aluminium hollow section joints based on the use of the hot spot stress method. The study includes experimental fatigue test data and analytical results, with a focus on the hot spot stress concentration factors (SCF_{hs}). A welded aluminium rectangular hollow section T-joint forms the basis of the study covering numerical stress analysis (finite element analysis); 3-D laser profile scanning of the welds; experimental stress analysis (strain gauges); and fatigue testing. Finite element analysis was performed on both idealised and actual (scanned) weld geometries. Values of SCF_{hs} were computed for three different load configurations and a comparison made of the effects of the idealised and scanned weld geometries. Differences ranging up to 17.5% were found from the variations in weld geometry alone. The dominant effect lay in the choice of Standards-based guidance for calculating the hot spot stress - causing variations as high as 38%. An experimental programme of some 40 new fatigue tests was compared with tentative design guidance previously drawn from earlier test results. The published database for RHS joints in aluminium remains small and further expansion of the database is clearly advantageous.

1 INTRODUCTION

Aluminium welded rectangular hollow section (RHS) joints are finding increased use in crane and bridge structures, transport vehicles and in automotive structures. Tubular structures are occasionally fabricated using forged or cast nodes but these are more expensive to produce than welded inter-tube connections which are consequently more common. However, the fatigue design basis for welded RHS joints in aluminium is limited [1,2]. An appropriate starting platform from which to establish a fatigue design methodology was thought to be the experience gained with similar structures fabricated in steel [3]. In particular, fatigue assessment based on the geometric hot spot stress range (or hot spot stress) concept [4] could potentially be adopted for aluminium structures. However, in automotive design the material thicknesses tend to be smaller than those used in civil engineering structures and this difference might limit the possibilities for transfer of data from the steel industry.

Earlier work on RHS joints in aluminium [5,6] examined stress concentration factors (SCFs) and defined preliminary design guidance from a modest series of fatigue tests. It was tentatively concluded [1] that a design *S-N* curve characterised by a FAT value of 40 (FAT is the stress range in MPa at 2×10^6 cycles, Figure 1) and an inverse slope of 3 could be used (Figure 2).

This paper presents some of the later work from these early studies - a study of the fatigue properties of welded aluminium RHS T-joints based on the use of the hot spot stress method. The objective is to better understand the SCFs and support the design *S-N* curve for these joints. Experimental fatigue test data and analytical results are described, with a focus on the hot spot stress concentration factors (SCF_{hs}). The programme of work covered finite element analysis (FEA); laser profile scanning of the welds; experimental stress analysis (strain gauges); and fatigue testing. The FEA was performed on both idealised and actual (scanned) weld geometries.

2 SPECIMEN PREPARATION

2.1 Fabrication

The rectangular hollow section (RHS) T-joint tested in this study was produced by a robotic gas metal arc welding (GMAW) process. Brace and chord structural elements were machined from the same series of extrusions, all of which were produced under identical manufacturing conditions at a single production facility. The extrusion alloy is 6060.35 T5 and welding consumables were 4043. The welded specimens consist of two identical RHS profiles with cross section dimensions of 40×60 mm, chord length of 500 mm, brace length of 250 mm and a wall thickness of 3 mm, Figure 3. Fully automated robotic welding was used to fillet weld the end of the brace to the flat side of the chord. In order to reduce distortion, the welding sequence around the circumference of the brace was split into two separate beads beginning at the same corner location, with welding proceeding in opposite directions around the joint meeting at the corner diagonally opposite. Welding parameters were 20.5-21.0 V, 132-140 A with travel speeds of 9-12 mms^{-1}.

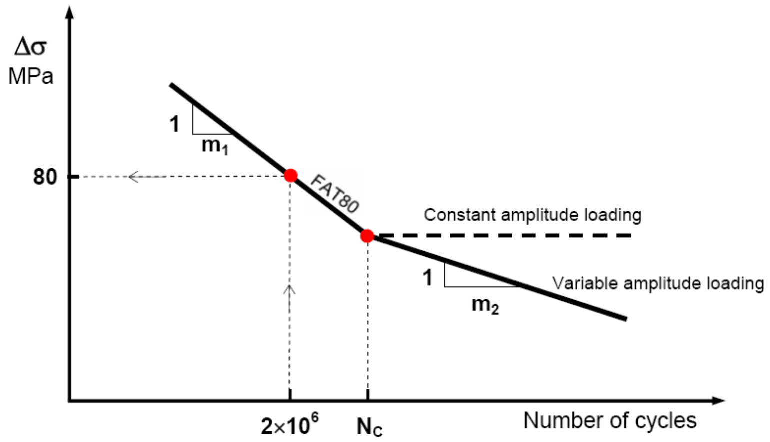

Figure 1 Characteristic *S-N* curves - FAT classification.

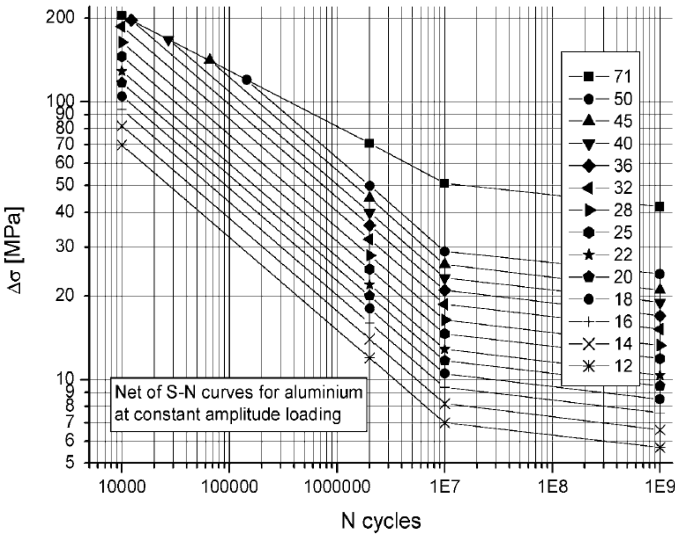

Figure 2 IIW *S-N* curves for aluminium [7].

The tensile properties of the weld metal and parent material are noted in Table I and the chemical composition of the base material in Table II, all obtained by analysis.

A small number of metallographic sections were taken from the welds for general investigation. The weld geometry was found to be rather variable with both root flaws and weld toe cold laps present, Figure 4. The latter occurring in steel joints have received much attention in the recent literature [10-12] and have a strong deleterious effect on fatigue strength for joints failing from the weld toe. Cold laps reduce the fatigue strength [10] since they act as sites for fatigue crack initiation, the crack growing from a cold lap quickly becoming normal to the applied stress / plate surface [11].

Table I Tensile properties [9].

Element	Alloy	$R_{p0.2}$ [MPa]	R_m [MPa]	A_5 [%]	Hardness [VHN_1]
Parent material	6060 T5	170	203	18.8	74
HAZ		64	152	26.3	68
Weld metal	4043	82	173	22.1	48

Table II Chemical composition (wt%).

Fe	Si	Cu	Mg	Cr	Mn	Zn	Zr
0.191	0.406	0.00879	0.467	0.00374	0.0152	0.00072	0.00185

Ti	Ni	B	Ga	Li	Na	Ca	Al
0.0128	0.00290	0.0009	0.0119	0	0.0005	<0.0001	98.82

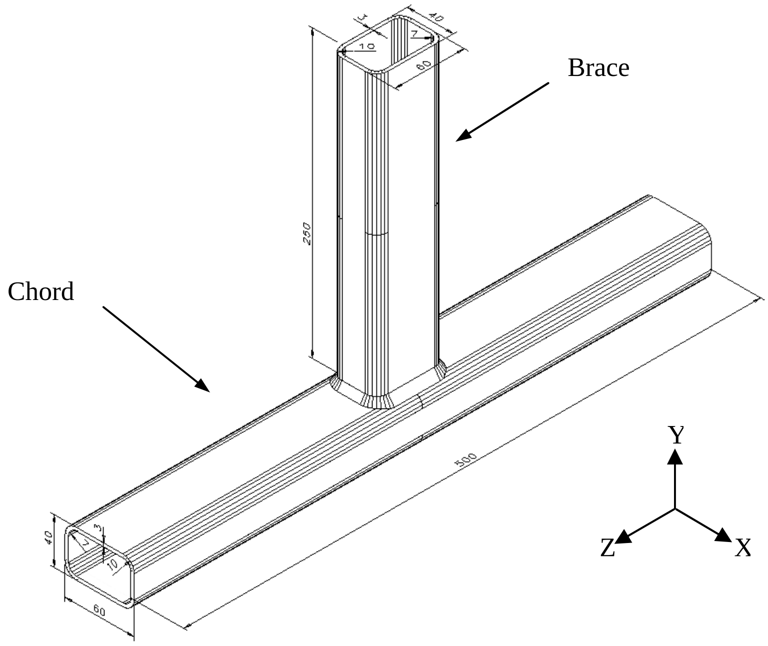

Figure 3 Geometry of welded RHS specimens, principal dimensions in mm.

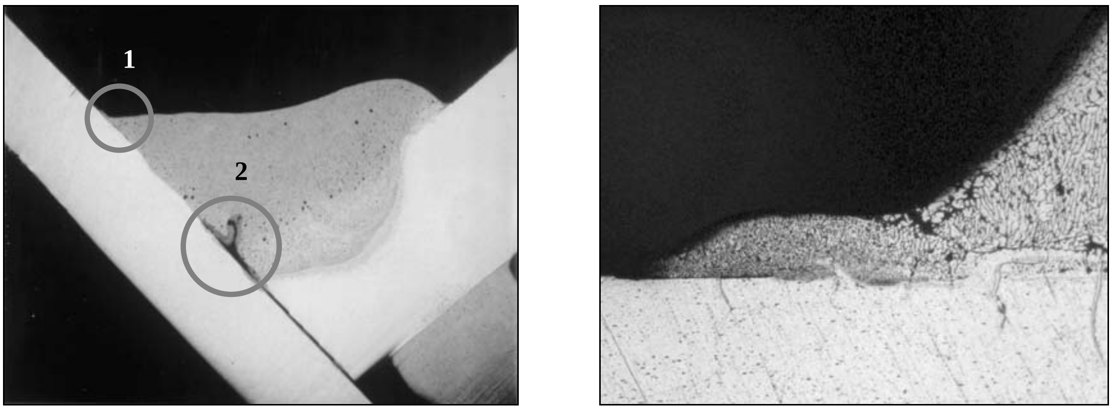

a) ×6

b) ×136

Figure 4 Variable weld geometry a) toe and root flaws, b) cold lap at site 1.

Lap-type fusion defects at weld toes in aluminium are believed to be caused by the presence of a surface oxide layer on the parent material with a considerably higher melting point (~2050°C) than metallic aluminium (~650°C). Since the temperature at the rim of the weld bead during welding is generally lower than the temperature of both the tip of the consumable electrode and the bulk of the weld pool, the temperature is probably insufficient to break down the oxide layer – incomplete fusion at the weld toe being the result.

2.2 Weld Characteristics

Profile scanning of the weld geometry was performed using a laser-based system. The same laboratory is now using a more advanced structured light system [8]. The aim was to scan the weld shape and transfer the information directly to generate an FE model based on the actual (measured) weld geometry. In this way the SCFs could be directly determined by analysis, rather than quantifying the notch effect in terms of local weld geometry features such as the weld toe radius, toe angle and leg length. More complete characterisation of the weld in terms of local geometric parameters has since been accomplished on similar specimens [2].

The laser scanning system used a moveable laser head and a rotating table to generate a point cloud representation of the weld with a point spacing of 0.5-1.0 mm in the horizontal plane and 0.5 mm vertically. These point data were then computer manipulated to produce surfaces suitable for transfer to the solid modelling and FE program, in this case I-DEAS.

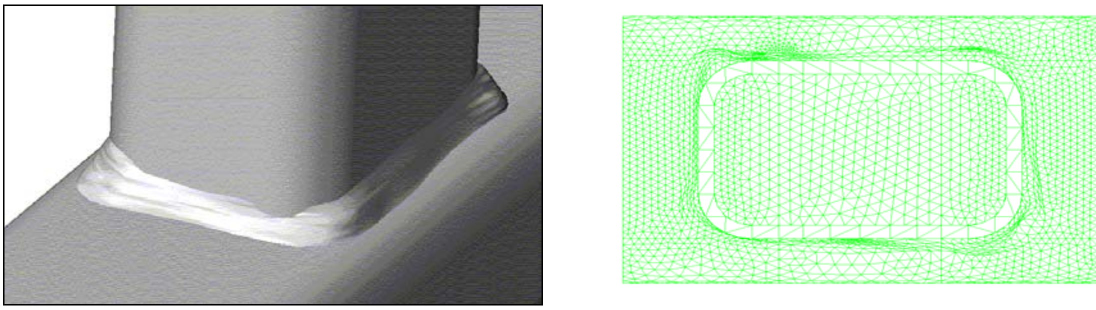

a) b)

Figure 5 Scanned geometry as a) solid model, b) finite element mesh.

2.3 Finite Element Analysis

Although a wider range of structural load configurations is of general interest, three important modes were selected: chord in four-point-bending; chord under axial load; and in-plane bending of the branch. The practicalities of building the FE model led to the adoption of 2nd order tetrahedral elements (10-noded). The models were also constructed to ease extraction of results at the locations required for determination of the hot spot values. Boundary conditions matched the experimental arrangements as closely as practicable and mesh optimisation was performed. Two models were constructed to represent the idealised and scanned geometries. The idealised weld geometry was a simple liner representation of the fillet weld with a flank angle of 55° to the chord axis and throat thickness of 3.5 mm.

The maximum longitudinal stress is located at the side corners due to the effect of shear lag. The specimen type examined in this study has two sides where fatigue failure may initiate at either side under the same nominal stress state (not the case for in-plane bending). A rigorous strategy was needed in order to obtain the hot spot stress extrapolation values from the FE results, particularly in cases where the uneven geometry of the scanned model complicated matters. The IIW recommendations [4] were used to select the extrapolation points while several numerical strategies were explored to obtain the corresponding stress values (nodes were not necessarily coincident with these extrapolation points). A logarithmic regression curve-fit to all nodal points on a line approaching the hot spot was found to give the optimum balance between ease of application and accuracy.

Table III Finite element results for hot spot stress

Load type	Model geometry	Hot spot (corner)	SCF_{hs}	Difference, %
4-point bending of chord	Idealised	-	2.27	Datum
	Scanned	1	2.22	-2.2
		2	1.93	-15.0
		3	2.26	-0.4
		4	1.98	-12.7
Axial loading of chord	Idealised	-	1.88	Datum
	Scanned	1	1.82	-3.1
		2	1.55	-17.5
		3	1.82	-3.2
		4	1.65	-12.2
In-plane bending of branch	Idealised	-	9.11	Datum
	Scanned	3	9.00	-1.2

The results are summarized in Table III in terms of maximum principal stress at the identical hot spots in the idealised geometry model (used as the reference value for comparisons), and the hot spots at each of the four unique corners in the scanned geometry model. Four-point bending was selected as the base case from which it is evident that corner 3 has the highest SCF of the four and was therefore used as the characteristic site for further comparisons. The largest deviation between idealized and scanned geometry is 17.5%. The location of the hot spot is the same for bending and axial loading of the chord. For in-plane bending however, the site moved further towards the outside of the joint, as seen in fatigue tests, Figure 8. A further comparison was made between several of the available strategies for extrapolation [7,13,14] applied to the worst case corner of the scanned model, Table IV. A logarithmic curve fit to the node path values for maximum principal stress was employed. Given the rapidly increasing stress gradients approaching the weld toe, it is not surprising that the methods that place the extrapolation points closer to the weld toe give correspondingly higher values of SCF_{hs}. The extreme variation is -38%.

Table IV Extrapolation method.

Load type	SCF_{hs} (% difference)			
	IIW / linear [7], Datum	IIW / quadratic [7]	DNV / linear [14]	van Wingerde / linear [13]
4-point bending, chord	2.27	2.39 (5.2)	2.16 (-4.8)	2.39 (-16.7)
Axial loading, chord	1.82	1.9 (4.3)	1.74 (-4.4)	1.56 (-14.3)
In-plane bending, branch	8.84	9.87 (11.7)	7.87 (-11.0)	5.48 (-38.0)

Notes:

Extrapolation method	Extrapolation point distances from weld toe, mm		
IIW / linear	1.2mm (**0.4t**)	3.0mm (**1.0t**)	
IIW / quadratic	1.2mm (**0.4t**)	2.7mm (**0.9t**)	4.2mm (**1.4t**)
DNV / linear	1.5mm (**0.5t**)	4.5mm (**1.5t**)	
van Wingerde / linear	4mm (**min. 4mm**)	5.8mm (**min. 4mm + 0.6t**)	

2.4 Strain Gauge Measurements

Measurements were made using specimens instrumented with single element strain gauges and gauge arrays placed at the hot spot locations relevant to the loading mode. The weld stop position was selected as the most severe of the four corners. The results are compared with FEA values extracted at the same locations. The FE results are here based on the axial coordinate stress component in order to better correspond with the strain gauge results.

Table V Comparison of SCFs from analysis (FEA) and experiment (strain gauges).

Load type	Analysis / measurement	Distance from weld toe*, mm	SCF_{hs}	Difference, %
4-point bending of chord	Strain gauge	2.0	2.27	Datum
	FEA	2.1	2.18	-4.0
		0.6	2.26	-0.4
Axial loading of chord	Strain gauge	2.0	2.03	Datum
	FEA	2.1	1.74	-14.3
		0.6	1.81	-10.8
In-plane bending of branch	Strain gauge	3.5	7.27	Datum
	FEA	3.5	7.48	2.9
		0.7	8.62	18.6

* Distance to first measurement point.

3 FATIGUE TESTING

A total of 40 fatigue specimens were available for testing. The tests were conducted in three load configurations matching those used in the FE study: 4-point bending of the chord; axial loading of the chord; and in-plane bending of the brace. The loading was provided by a servo-hydraulic actuator mounted in a test frame. Sinusoidal constant amplitude loading at R = 0.1 was applied and the testing performed under in-air laboratory conditions at ambient temperature. Load frequency lay in the range 5-15 Hz, dependent upon the level of applied load and the test configuration. The number of tests and load levels were chosen based on ASTM E739 guidance. The aim was to establish results in the range from 5×10^4 to 5×10^6 cycles. Tests were unambiguously continued until total loss of load-carrying capacity.

3.1 Fatigue test results

Of the 40 tests, two run-outs occurred and four tests were discarded on account of failure in the grips or equipment malfunction, Table VI. The fatigue test results are given in Table VII expressed in terms of nominal stress range. The data and mean regression lines for the three test arrangements show that the in-plane branch bending case is clearly differentiated from the chord loaded cases, Figure 6. This is supported by the clear shift of crack initiation site observed in the tests, Figure 8, and suggested by the FE results. Re-evaluating the results in terms of the relevant hot spot stress range for each load configuration brings the three data sets together, Figure 7. The SCF_{hs} values are taken from the FEA of the scanned geometry, Table **III**. Both the SCF_{hs} values used for the two chord-loaded cases (2.24 for bending, 1.82 for axial load) were derived by averaging the two corner results for the weld stop- and start-positions because fatigue cracks consistently initiated at these two sites during testing. The non-symmetric nature of loading of the in-plane bending case meant that just the single weld-stop corner was relevant as the site of initiation – where SCF_{hs} = 9.0). Load shedding behaviour was evident for the in-plane bending tests. Crack initiation invariably began at the corner containing the weld stop, but once the fatigue crack developed to approximately full thickness through the chord, a second crack initiated at the adjacent corner, but on the upper weld toe, growing into the brace.

Table VI Summary of tests

Load type	Number of specimens	Number failing at weld start corner	Number failing at weld stop corner
4-point bending of chord	13	10	3
Axial loading of chord	10	8	2
In-plane bending of branch	11	11	Not tested

Table VII Fatigue test data (nominal stress)

Four-point bending, chord		Axial loading, chord		In-plane bending, branch	
Stress range [MPa]	Endurance, cycles	Stress range [MPa]	Endurance, cycles	Stress range [MPa]	Endurance, cycles
111.04	54834	121.10	58162	32.29	48768
111.04	58447	121.10	46681	29.46	80631
111.04	90029	110.72	69233	29.46	97158
98.70	74830	86.50	138616	24.93	230602
98.70	83700	86.50	171144	24.93	211347
82.25	121459	69.20	443078	21.53	341207
82.25	362667	69.20	503841	21.53	403047
82.25	375984	51.90	1473611	18.70	728744
65.80	443461	51.90	1197103	18.01	772575
65.80	466329	44.98	1656890	15.51	3247211
49.35	1958545	44.98	*5E+6	15.51	2343425
49.35	2199480				
41.13	7487410				
41.13	*1.55E+7				

* denotes run-out

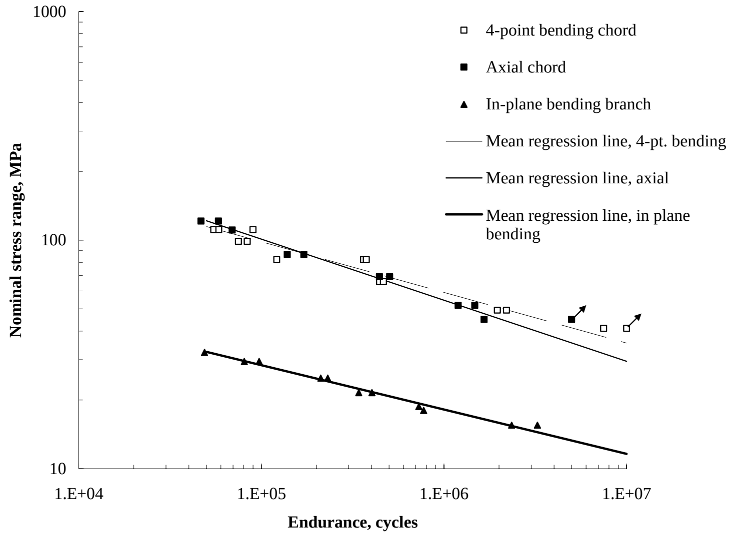

Figure 6 Fatigue test results (nominal stress) with mean regression lines.

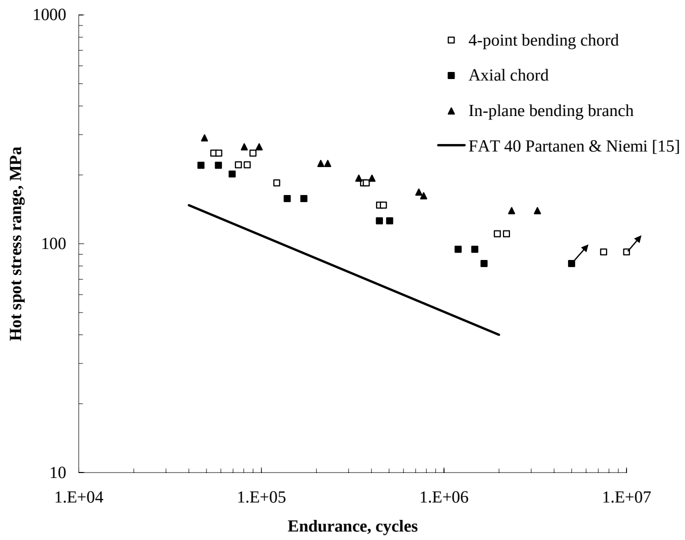

Figure 7 Fatigue test results (hot spot stress) with FAT 40 design curve.

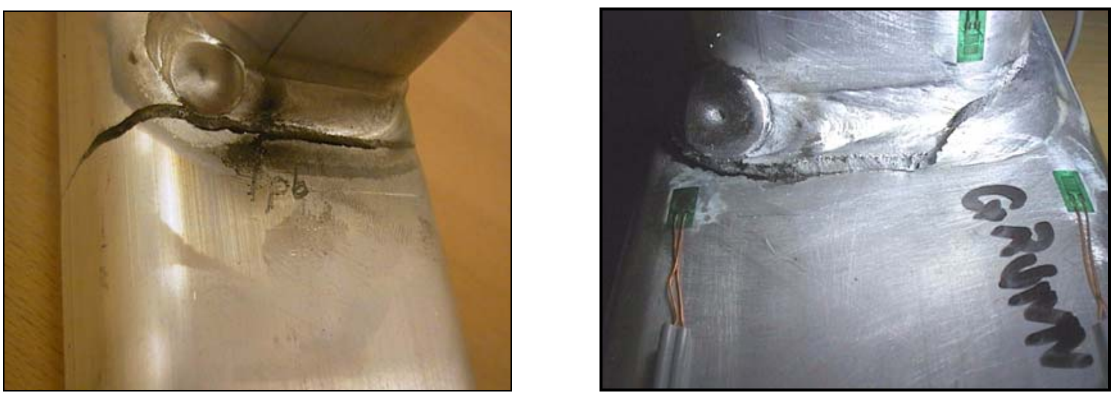

a) b)

Figure 8 Fatigue crack initiation a) corner and weld stop position in chord-loaded tests and b) double initiation sites for in-plane bending tests.

Evaluation of the published literature has previously recommended the use of the IIW definitions and FE procedures for hot spot stress analysis [1]. Largely due to the small database, a tentative suggestion was made to use the Partanen and Niemi hot spot S-N curve (based on welds in aluminium) with a FAT value of 40 and an inverse slope of 3, plotted here with the present results Figure 7. The published experimental fatigue database for RHS joints in aluminium is still small, and although the present data lie comfortably above the recommended design line, it remains prudent to recommend the FAT 40 design line until a more comprehensive design basis is established.

4 CONCLUSIONS

Values of SCF_{hs} were computed by FEA for three different load configurations and a comparison made of the effects of the idealised and scanned weld geometries. However, the important outcome of this work is the expansion of the published fatigue test database. The following points are noted:

- Variations in SCF_{hs} of 17.5% were found between the idealised and scanned geometries. The dominant effect lay in the choice of Standards-based guidance for calculating the hot spot stress - causing variations of 38%.
- An experimental programme of some 40 fatigue tests was compared with tentative design guidance previously drawn from earlier test results, further supporting the FAT 40 classification as a design line.
- The published database for RHS joints in aluminium remains small and further expansion of the design basis is clearly needed if any improvement of the FAT 40 design line is to be justified.

ACKNOWLEDGEMENTS

The authors wish to acknowledge the work and contributions of laboratory staff and undergraduate students at NTNU, in particular Thomas Haavi.

REFERENCES:

1. K. A. Macdonald and P. J. Haagensen, *Engineering Failure Analysis*, 6, (1999), 113-130.
2. B.W. Tveiten et al., *International Journal of Fatigue*, 28, (2006), 1667–1676.
3. X.-L. Zhao and J. A. Packer, Recommended fatigue design procedure for welded hollow section joints, IIW doc. XIII-1772-99 / XV-1021-99. Abington Publishing, Abington, Cambridge, UK, 2000, ISBN 1-85573-522-9.
4. E. Niemi, W. Fricke and S. J. Maddox, Fatigue analysis of welded components – designer's guide to the structural hot-spot stress approach, IIW doc. XIII-1819-00 / XV-1090-01, update June 2003, Woodhead Publishing, Cambridge, UK, 2006, ISBN 1-84569-124-5.
5. R. M. Edvardsen and R. Trandum, Fatigue of welded rectangular aluminium hollow section joints, Master's Thesis, Norwegian University of Science and Technology, 1996.
6. T. Haavi, Fatigue of welded joints in extruded aluminium hollow section profiles, Master's Thesis, Norwegian University of Science and Technology, 1998.
7. A. Hobbacher, Recommendations for fatigue design of welded joints and components, IIW doc. XIII-2151-07 / XV-1254-07.
8. F. Couweleers, Ø. Skotheim and B. W. Tveiten, Eighth international symposium on measurement and quality control in production, Erlangen, Germany, October 12–15; 2004.
9. J. Ødegård, Z. Zhang and A. O. Kluken, International body engineering conference, Germany, 1997.
10. J. Samuelsson, Design and analysis of welded high strength steel structures, Stockholm, Sweden, EMAS Ltd.; 2002, p. 151–61.
11. J. Martinsson, Design and analysis of welded high strength steel structures, Stockholm, Sweden, EMAS Ltd.; 2002, p.163–84.
12. J. Samuelsson, International symposium on integrated design and manufacturing of welded structures, Eskilstunet, Sweden, March 13-14, 2007, ISBN 978-952-214-363-1.
13. A. M. van Wingerde et al, The fatigue behaviour of K-joints made of square hollow sections, IIW doc. XIII-1626-96 / XV-913-96 / XV-E-96-233.
14. DNV RP-C203, Fatigue design of offshore steel structures, Det Norske Veritas, Norway, 2005.
15. T. Partanen and E. Niemi, Hot spot S-N curves based on fatigue tests of small MIG welded aluminium specimens, IIW doc. XIII-1636-96.